Available online at www.sciencedirect.com
ScienceDirect
Trans. Nonferrous Met. Soc. China 28(2018) 2360−2367
Transactions of Nonferrous Metals Society of China
www.tnmsc.cn

A clean process of lead recovery from spent lead paste based on hydrothermal reduction

Wei-feng LIU[1,2], Xun-bo DENG[1], Du-chao ZHANG[1], Tian-zu YANG[1], Lin CHEN[1]

1. School of Metallurgy and Environment, Central South University, Changsha 410083, China;
2. Henan Yuguang Gold and Lead Group Co., Ltd., Jiyuan 459000, China

Received 2 August 2017; accepted 18 April 2018

Abstract: An innovative process was proposed for recovering lead from spent lead paste, and it produced less pollution and used less energy than the traditional process. First, lead dioxide in lead paste was reduced by glucose under hydrothermal conditions. The effects of the reaction time, glucose excess coefficient, temperature and pH on the hydrothermal reduction were systematically investigated. Under the optimized reduction conditions (i.e., temperature of 175 °C, time of 120 min, glucose excess coefficient of 3.0 and pH of 5.5), 99.9% reduction ratio of lead dioxide is achieved, and only the $PbO{\cdot}PbSO_4$ and $PbSO_4$ phases are observed in the reducing residue. Subsequently, the reducing residue is desulfurized in a NaOH solution, and approximately 99.40% of the sulfur is removed. The main lead phase in the desulfurization residue is $3PbO{\cdot}H_2O$.

Key words: spent lead paste; hydrothermal reduction; glucose; desulfurization

1 Introduction

Lead is a non-ferrous metal with special physical and chemical properties, which is widely used to prepare alloys. Lead acid batteries represent the most important application of lead, accounting for more than 80% of the total lead consumption in the world [1]. Lead acid batteries are inexpensive, and their technology is mature with a good safety performance. They are widely used in many fields, such as automobiles, electric vehicles, and energy storage [2−6]. Lead acid batteries occupy more than 70% of the global secondary battery market share [7]. Correspondingly, spent lead acid batteries dominate the raw materials of the secondary lead, accounting for over 85% of the wastes [8]. Thus, spent lead acid batteries can be viewed as the most important renewable lead resources.

If being treated inappropriately, spent lead acid batteries can cause serious environmental pollution because they contain large amounts of hazardous substances, such as lead and sulfuric acid [9]. Spent lead acid batteries are usually dismantled and then recovered. There are four main components of the dismantled products: polymeric containers, lead alloy grids, paste and waste acid. Among these, spent lead paste is the most difficult component to treat [10−12]. The lead paste consists of lead sulfate, lead dioxide, lead oxide and a small amount of metallic lead [13]. Usually, lead is recovered from the lead paste using pyrometallurgical or hydrometallurgical processes.

During the pyrometallurgical process, lead paste is usually individually melted or mixed with lead concentrate in a reverberatory furnace, blast furnace, or oxygen bottom blowing furnace to produce crude lead and then electrolyzed to produce cathode lead [14]. Pyrometallurgical processes are quick and allow for a large throughput. However, they consume a substantial amount of energy and emit harmful sulfur oxides and lead-contained particulates, which constrain their applications.

A large amount of research has been conducted to seek a hydrometallurgical approach to recover lead from lead paste. Conventional hydrometallurgy processes mainly comprise three steps: (1) desulfurizing lead sulfate and reducing PbO_2 to Pb^{2+}; (2) dissolving the

Foundation item: Project (2016M602427) supported by the Postdoctoral Science Foundation of China; Project (51504292) supported by the National Natural Science Foundation of China; Project (2016zzts288) supported by Graduate Student Innovation Foundation of Central South University, China

Corresponding author: Du-chao ZHANG; Tel: +86-13787003744; E-mail: zdc015@sina.com

DOI: 10.1016/S1003-6326(18)64881-2

transformation slag in leaching solutions, such as HBF_4 and H_2SiF_6; (3) producing metallic lead by electro-winning [15−17]. Although this solves the problems associated with emissions of SO_2 and lead particulates, it still has the shortcomings of a long flowsheet and high energy consumption. Another hydrometallurgy process for treating lead paste without electrowinning uses citrate acid and sodium citrate to generate a lead citrate precursor; then, lead is recovered after calcining the lead citrate precursor [18,19]. However, its high reagent costs and slow reaction rate limit its widespread application.

The key points are to efficiently achieve eco-friendly removal of sulfate and reduction of lead dioxide in lead paste. There are many studies on the reduction of lead dioxide in waste lead paste; the commonly used reagents contain H_2O_2(aq), $FeSO_4$ and $Na_2S_2O_3$. These industrial chemicals are usually unstable and require specific reduction conditions, providing a low reduction efficiency. However, glucose is a naturally occurring green reducing agent that is inexpensive and shows stable chemical properties.

Hydrothermal methods refer to chemical reactions that use water as the solvent in a sealed pressure vessel under high-temperature and high-pressure conditions. These methods have been widely applied in the fields of metallurgy and advanced materials preparation, e.g., the reduction of nickel oxide to prepare high-purity nickel powder under hydrothermal conditions [20]. Additionally, ferric hydroxide has been reduced to ferric oxide under hydrothermal conditions using glucose, starch and urea as the reducing agents [21,22].

Based on the aforementioned analysis, we propose a new process for recovering lead form lead paste. First, lead dioxide in the lead paste was reduced to lead oxide using glucose under hydrothermal conditions; then, sodium hydroxide was used to desulfurize the reducing residue and convert all lead phases to lead oxide. The effects of reaction time, glucose excess coefficient, pH and temperature on the glucose hydrothermal reduction were studied in detail.

2 Experimental

2.1 Experimental materials

Spent lead paste was provided by Henan Yuguang Gold and Lead Co., Ltd. (China). Before the hydrothermal reduction process, the lead paste was washed with distilled water to remove any remaining sulfuric acid. The simples were then dried, ground and sieved until their particle sizes were below 74 μm. The chemical composition and X-ray diffraction (XRD) pattern of the fine lead paste are given in Table 1 and Fig. 1, respectively. The lead paste mainly contains elemental lead and sulfur, and the major lead phases in the lead paste are $PbSO_4$, PbO_2 and PbO.

Table 1 Chemical composition of fine lead paste (mass fraction, %)

$PbSO_4$	PbO_2	PbO	Pb	S	Total lead
57.82	29.73	9.88	1.31	6.05	75.75

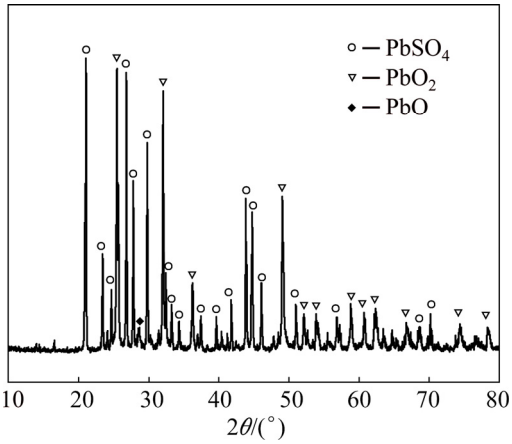

Fig. 1 XRD pattern of fine lead paste

A scanning electron microscopy−energy dispersive X-ray spectroscopy (SEM−EDS) image of the lead paste is shown in Fig. 2. Various particle sizes are present in the lead paste, and the main elements are lead and sulfur; however, different areas show different lead and sulfur contents.

2.2 Experimental fundamentals

During the hydrothermal reduction process, the lead dioxide and glucose are defined as the oxidant and reductant, respectively. During the desulfurization process, the lead sulfate is transformed to lead oxide in a sodium hydroxide solution [23]. The main chemical reactions can be expressed as follows:

$$C_6H_{12}O_6\cdot H_2O(aq)+12PbO_2(s)\rightarrow 12PbO(s)+6CO_2(g)+7H_2O(l) \quad (1)$$

$$PbSO_4(s)+2NaOH(aq)\rightarrow PbO(s)+Na_2SO_4(aq)+H_2O(l) \quad (2)$$

2.3 Experimental procedure

The hydrothermal reduction was carried out in a 250 mL stainless steel autoclave. First, a quantitative glucose solution and lead paste were added to the autoclave at a certain molar ratio of $C_6H_{12}O_6\cdot H_2O$ to PbO_2. Next, the stirrer and heater were turned on. After the reaction, the stirrer and heater were turned off, and the autoclave was cooled naturally. When the temperature decreased below 60 °C, the slurry was removed from the autoclave, and it was filtered using a vacuum pump. Finally, the filter cake was dried at 80 °C,

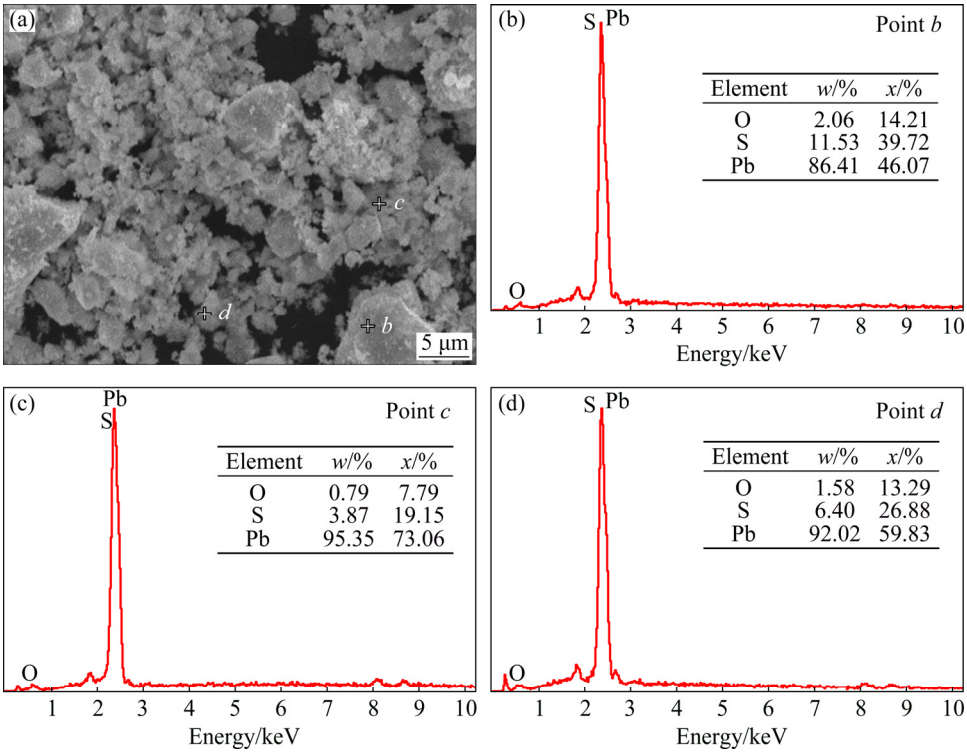

Fig. 2 SEM micrograph of lead paste sample (a) with EDS analysis of selected areas (b−d)

and the content of lead dioxide was analyzed by chemical phase analysis. The reduction ratio of lead dioxide was calculated using

$$R = 1 - \frac{M_r \times w_r}{M_m \times w_m} \quad (3)$$

where M_r and M_m are the masses of the reducing residue and lead paste, respectively, and w_r and w_m are the contents of lead dioxide in the reducing residue and lead paste, respectively.

2.4 Analysis and characterization

The contents of the lead phases in the lead paste and reducing residue were determined by chemical titration. The sulfur content in the lead paste and desulfurization residue were quantitatively determined using a high-frequency infrared carbon & sulfur analyzer (CS844, LECO Corporation). The phases of the solid sample were identified by XRD using a Rigaku TTRAX−3 instrument (40 kV, 30 mA, 10 (°)/min). The microstructures were characterized using a JEOL JSM−6360LV scanning electron microscope equipped with an EDS system (EDX-GENESIS 60 S, EDAX, USA) for microanalysis at an accelerating voltage between 0.5 and 30 kV.

3 Results and discussion

3.1 Choice of reducing agent

The reduction ratios of lead dioxide in lead paste using various reductants are given in Table 2. All the experiments were performed under optimal conditions according to a previous study [24], except using glucose as the reducing agent.

Table 2 Reduction effect of various reducing agents

Reducing agent	Excess coefficient	Reduction ratio/%
H_2O_2	6.4	45.24
$Na_2S_2O_3$	9.6	78.95
Na_2SO_3	6.4	62.07
$FeSO_4$	12	96.48
$H_2C_2O_4$	4	97.12
$C_6H_{12}O_6{\cdot}H_2O$	2	97.76

The reduction ratio of lead dioxide is lower when H_2O_2, $Na_2S_2O_3$ or Na_2SO_3 is used as the reducing agent (Table 2). Moreover, the instability of H_2O_2 and $Na_2S_2O_3$ increases the consumption of the reagent. A disproportionation reaction can occur in the Na_2SO_3 solution to generate sulfion [24], which could react with $PbSO_4$ to form PbS, abating lead recovery and increasing consumption of the reagent. Lead dioxide is thoroughly reduced using $FeSO_4$ as the reductant; however, the reduction reaction only occurs in a sulfuric acid system, producing lead sulfate, which must be desulfurized in the following process. Both oxalic acid and glucose are highly-efficient and green reductants that do not produce pollution, but glucose is a more cost-effective reductant. Therefore, it is necessary to study the reduction process

of lead dioxide by glucose in detail.

3.2 Effect of time

The effect of time on the reduction ratio of lead dioxide was studied from 15 to 180 min under the following initial conditions: 20 g lead paste, temperature of 150 °C, glucose excess coefficient of 3.0, pH of 5.5, liquid-to-solid ratio (L/S) of 10/1, and stirring rate of 600 r/min. The results are shown in Fig. 3.

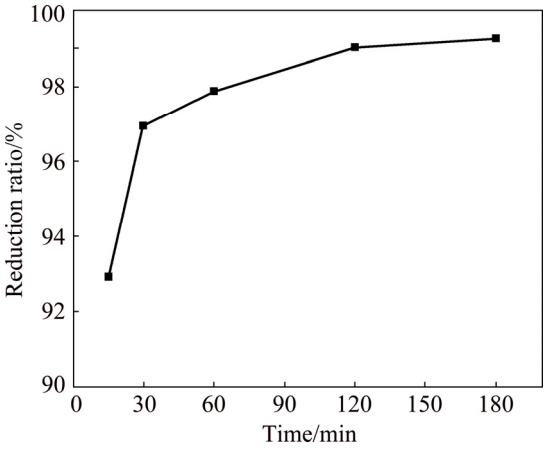

Fig. 3 Effect of time on reduction ratio of PbO_2

Figure 3 shows that the reduction ratio of lead dioxide is affected by the reaction time. When the reaction time is 15 min, the reduction ratio reaches 92.93%, indicating that the reaction rate is very fast. As the reaction time increases from 15 to 120 min, the reduction ratio of lead dioxide increases from 92.93% to 99.03%. With longer reaction time, the change in the reduction ratio of lead dioxide is negligible.

The XRD pattern of the reducing residue at various reaction time is shown in Fig. 4. The peak of PbO_2 disappears at different reaction time, which is consistent with the results in Fig. 3. New peaks of $PbO{\cdot}PbSO_4$ appear for the residue, indicating that PbO obtained from the reduction of PbO_2 further reacts with $PbSO_4$ in the lead paste. The reaction can be described as follows:

$$PbO(s)+PbSO_4(s)\rightarrow PbO{\cdot}PbSO_4(s) \quad (4)$$

The characteristic peaks of susannite ($2PbCO_3{\cdot}PbSO_4{\cdot}Pb(OH)_2$) are observed in the XRD patterns at different time, and their intensities gradually decrease. The reason might be that the decomposition product (CO_2) of glucose dissolves in water to form CO_3^{2-}, and then reacts with PbO and $PbSO_4$ in the system to form susannite. However, with increasing the reaction time, susannite decomposes again. The formation of $2PbCO_3{\cdot}PbSO_4{\cdot}Pb(OH)_2$ can be expressed according to Eq. (5). Therefore, to improve the efficiency and avoid the production of the intermediate product, a reaction time of 120 min was used.

$$3PbO(s)+PbSO_4(s)+2CO_2(g)+H_2O(l)\rightarrow 2PbCO_3{\cdot}PbSO_4{\cdot}Pb(OH)_2(s) \quad (5)$$

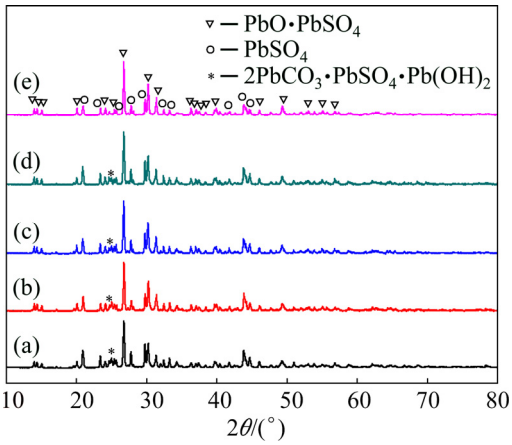

Fig. 4 Effect of time on XRD pattern of reducing residue: (a) 15 min; (b) 30 min; (c) 60 min; (d) 120 min; (e) 180 min

3.3 Effect of excess coefficient of glucose

The excess coefficient of glucose was calculated according to Eq. (1). Experiments were performed to test the effect of the amount of glucose on the reduction ratio of lead dioxide under the following conditions: 20 g lead paste, temperature of 150 °C, pH of 5.5, initial L/S of 10/1, stirring rate of 600 r/min, and reaction time of 120 min. The results are shown in Fig. 5.

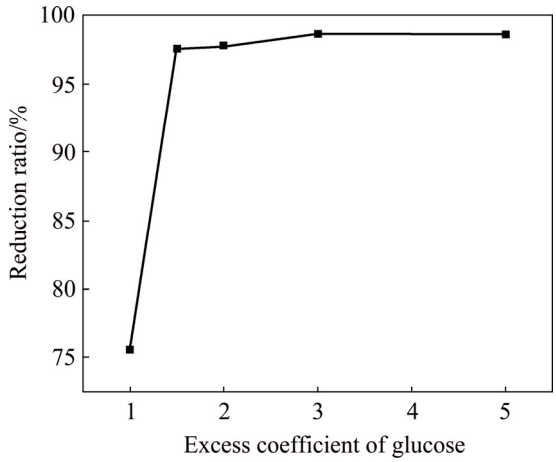

Fig. 5 Effect of excess coefficient of glucose on reduction ratio of PbO_2

When the excess coefficient of glucose increases from 1.0 to 1.5, the reduction ratio of lead dioxide rapidly increases from 75.56% to 97.55% (Fig. 5). However, the reduction ratio remains nearly constant when the excess coefficient of glucose is above 1.5.

Figure 6 displays the effect of different excess coefficients of glucose on the XRD pattern of the reducing residue. The peaks of PbO_2 and $2PbCO_3{\cdot}PbSO_4{\cdot}Pb(OH)_2$ are visible in the XRD pattern of the

reducing residue when the glucose excess coefficient is 1.0, which indicates that a low amount of glucose reduces the reduction ratio and produces intermediate products. By improving the excess coefficient of glucose, the PbO_2 peak quickly disappears and the peak intensity of $2PbCO_3·PbSO_4·Pb(OH)_2$ gradually weakens. Therefore, an excess coefficient of glucose of 3.0 is appropriate to improve the reduction ratio and reduce the generation of intermediate products.

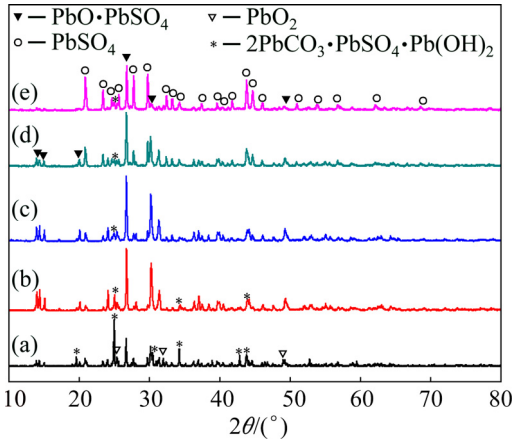

Fig. 6 Effect of excess coefficient of glucose on XRD pattern of reducing residue: (a) 1; (b) 1.5; (c) 2; (d) 3; (e) 5

3.4 Effect of pH

Experiments were performed to test the effect of different pH values on the reduction ratio of lead dioxide under the following conditions: 20 g lead paste, temperature of 150 °C, glucose excess coefficient of 3.0, initial L/S of 10/1, stirring rate of 600 r/min, and reaction time of 120 min. The pH was adjusted to acidic or alkaline by adding sulfuric acid or ammonia. The results are shown in Fig. 7.

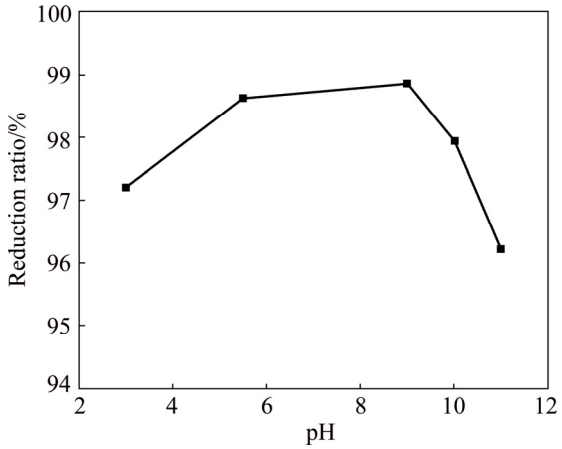

Fig. 7 Effect of pH on reduction ratio of PbO_2

The reduction ratio of lead dioxide is above 95% at different pH values, indicating that the reduction effect of glucose is less affected by the reaction system (Fig. 7). The reduction ratio increases slowly from 97.20% to 98.86% with the increase in pH from 3.0 to 9.0. However, the reduction ratio decreases as the pH value continues to increase.

The effect of pH on the XRD pattern of the reducing residue is shown in Fig. 8. No PbO_2 peaks are visible in the reducing residue at different pH values. This is consistent with the reduction ratio shown in Fig. 7, indicating that the reduction process is completed. The peak intensity of $2PbCO_3·PbSO_4·Pb(OH)_2$ decreases gradually with increasing pH; at a pH of 10, the peak completely disappears. This illustrates that properly increasing the pH value can promote decomposition of $2PbCO_3·PbSO_4·Pb(OH)_2$. Considering the reduction ratio and reagent consumption, an initial pH of 5.5 is chosen.

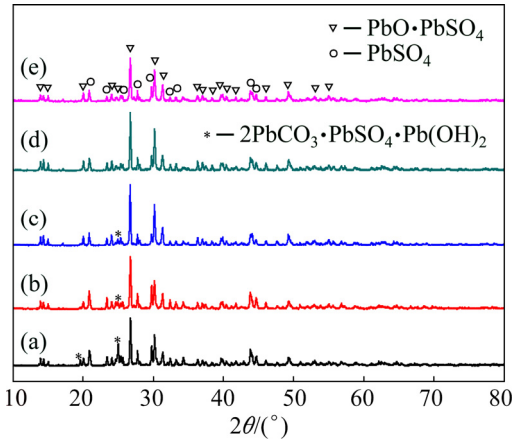

Fig. 8 Effect of pH on XRD pattern of reducing residue: (a) 3; (b) 5.5; (c) 9; (d) 10; (e) 11

3.5 Effect of temperature

Experiments were performed to investigate the effect of a temperature change on the reduction efficiency under the following conditions: initial L/S of 10/1, 20 g lead paste, glucose excess coefficient of 3.0, initial pH of 5.5, stirring rate of 600 r/min, and reaction time of 120 min. The results are displayed in Fig. 9.

The reduction ratio of lead dioxide increases sharply from 65.77% to 97.44% when the temperature increases from 100 to 125 °C (Fig. 9). When the temperature is 175 °C, the reduction ratio reaches 99.9%. The results indicate that higher temperatures improve the reduction ratio.

The effects of temperature on the XRD pattern of the reduction residue are shown in Fig. 10. Peaks of PbO_2 are present at 100 °C, which further indicates that the reduction of PbO_2 is not complete at the lower temperature (Fig. 10). When the temperature increases from 100 to 150 °C, the peak of $2PbCO_3·PbSO_4·Pb(OH)_2$ is present. When the temperature continuously increases to 175 °C, the peak of $2PbCO_3·PbSO_4·$

$Pb(OH)_2$ completely disappears, indicating that the higher temperature increases the reduction ratio and eliminates the intermediate product. Therefore, 175 °C is chosen as the optimal temperature.

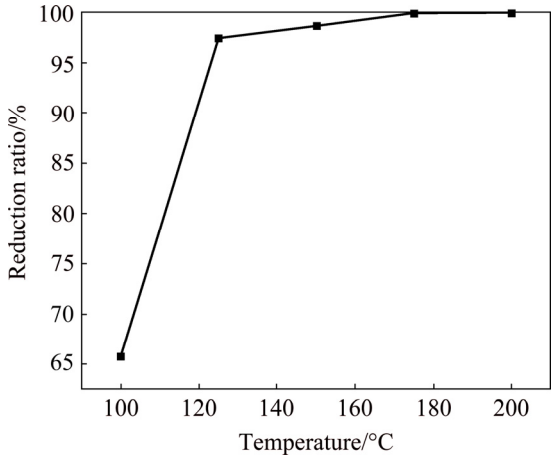

Fig. 9 Effect of temperature on reduction ratio of PbO_2

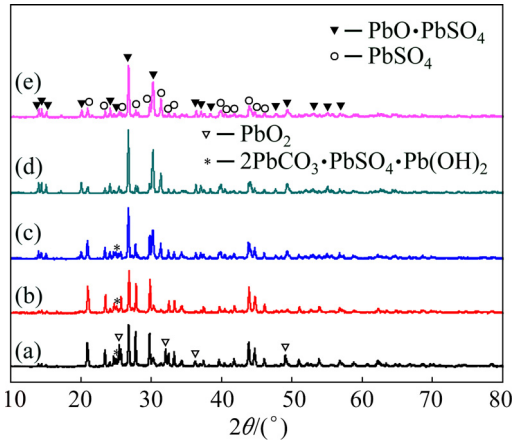

Fig. 10 Effect of temperature on XRD pattern of reducing residue: (a) 100 °C; (b) 125 °C; (c) 150 °C; (d) 175 °C; (e) 200 °C

3.6 Optimal reduction conditions

Based on the above single-factor experiments, the following optimal conditions are identified: glucose excess coefficient of 3.0, initial pH of 5.5, stirring rate of 600 r/min, initial L/S of 10/1, temperature of 175 °C and reaction time of 120 min. Under these conditions, the reduction ratio of lead dioxide reaches 99.9%. The main chemical composition of the reducing residue is given in Table 3.

Table 3 shows that the contents of total lead and sulfur do not substantially change, and lead dioxide is no longer present in the reducing residue. The content of lead oxide substantially increases, indicating a thorough reducing process. The XRD pattern of the reducing residue (Fig. 10(d)) demonstrates that the main phase compositions are $PbO{\cdot}PbSO_4$ and $PbSO_4$. The SEM−EDS analyses of the reducing residue are shown in Fig. 11. The image shows that the morphology of the reduction residue significantly changes with respect to that of the lead paste.

Table 3 Chemical composition of reducing residue (mass fraction, %)

$PbSO_4$	PbO	Pb	S	Total lead
59.13	38.39	1.22	6.25	77.26

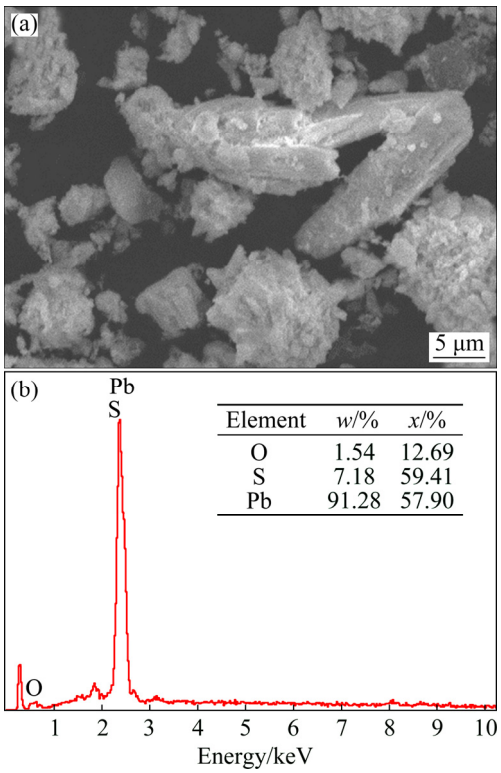

Fig. 11 SEM micrograph of reducing residue sample (a) with EDS analysis (b)

3.7 Desulfurization process

The reducing residue under optimal conditions and spent lead paste were desulfurized by reacting each with sodium hydroxide under the same conditions: 10 g reducing residue or lead paste, temperature of 50 °C, molar ratio of NaOH to $PbSO_4$ of 2.4:1, liquid-to-solid ratio of 5:1, stirring speed of 400 r/min, and reaction time of 1 h. The results of the desulfurization experiments are given in Table 4.

Table 4 shows that the desulfurization ratios for lead paste and the reduced residue are 97.48% and 99.40%, respectively. The difference occurs because a tiny fraction of lead sulfate is encapsulated by lead dioxide in the lead paste and cannot participate in the desulfurization process. However, the adverse effect can be eliminated when the reduced residue is adopted. The recovery efficiencies of lead during the desulfurization process from lead paste and the reduced residue are

97.90% and 97.54%, respectively. The decrease is caused by the dissolution of lead oxide in sodium hydroxide:

$$PbO(s)+NaOH(aq)\rightarrow NaHPbO_2(aq) \quad (6)$$

Table 4 Results of desulfurizing process for lead paste and reduced residue

Parameter	Lead paste	Reduced residue
Mass of residue/g	8.47	8.35
Lead content in residue (mass fraction)/%	87.56	90.25
Sulphur content in residue (mass fraction)/%	0.18	0.045
Lead content in filtrate/(g·L^{-1})	2.51	2.93
Desulfurization ratio/%	97.48	99.40
Lead recovery efficiency/%	97.90	97.54

The phases and morphology of the desulfurized paste from the reducing residue were determined by XRD and SEM−EDS analyses, respectively. As shown in Fig. 12, $3PbO·H_2O$ is the only phase in the desulfurized paste. The chemical analysis provides a lead content of 90.25%, which is consistent with the theoretical lead content of $3PbO·H_2O$ (90.39%). Figure 13 shows that the morphology of the desulfurized paste is more regular than that of the reducing residue, but there are still many agglomerated crystals. The EDS pattern shows that the desulfurized residue does not contain sulfur, which is consistent with the chemical analysis.

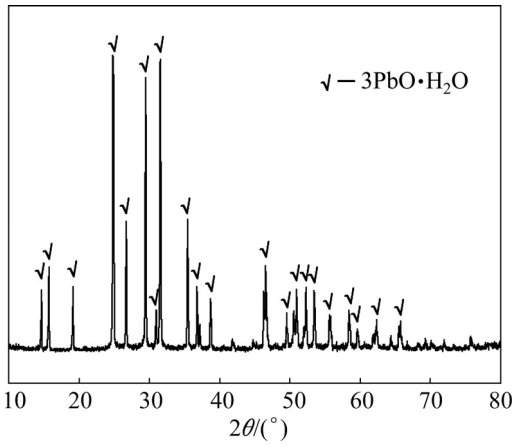

Fig. 12 XRD pattern of desulfurized paste

4 Conclusions

1) To achieve the complete removal of sulfate and the reduction of lead dioxide in lead paste, lead dioxide should be first reduced by glucose under hydrothermal conditions. Then, the reduced lead paste could be desulfurized using sodium hydroxide.

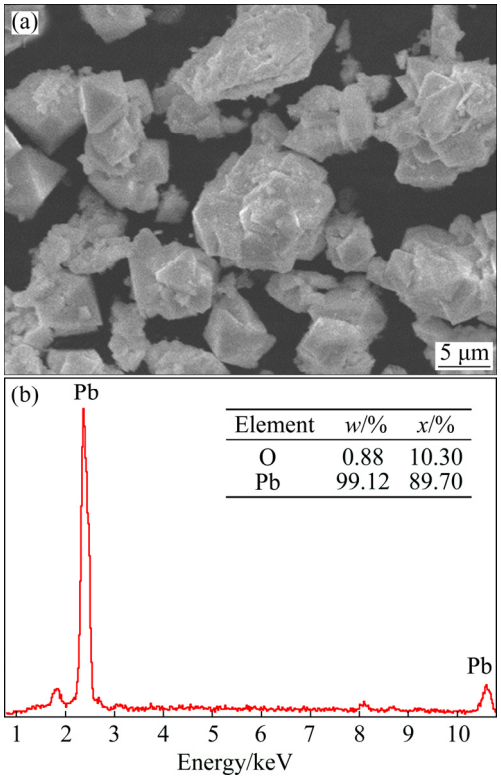

Fig. 13 SEM micrograph of desulfurized paste (a) with EDS analysis (b)

2) The following optimal reduction conditions are determined: glucose excess coefficient of 3.0, initial pH of 5.5, temperature of 175 °C, and reaction time of 120 min. Under these conditions, the reduction ratio of lead dioxide reaches 99.9%, and the main phases in the reducing residue are $PbSO_4$ and $PbSO_4·PbO$.

3) Under optimal conditions, the reducing residue and spent lead paste are each desulfurized by reacting with sodium hydroxide. The desulfurization ratios are 99.40% and 97.48%, respectively, indicating that complete reduction of lead dioxide in spent lead paste is beneficial to the subsequent desulfurization.

References

[1] ZHU Xin-feng, LIU Wan-chao, YANG Hai-yu, LI Lei, YANG Jia-kuan. Preparation of ultrafine PbO powders from lead paste in spent lead acid battery [J]. The Chinese Journal of Nonferrous Metals, 2010, 20(1): 132−136. (in Chinese)

[2] PAN Jun-qing, ZHANG Chao, SUN Yan-zhi, WANG Zi-hao, YANG Yu-sheng. A new process of lead recovery from waste lead-acid batteries by electrolysis of alkaline lead oxide solution [J]. Electrochemistry Communications, 2012, 19: 70−72.

[3] REZAEI B, MALLAKPOUR S, TAKI M. Application of ionic liquids as an electrolyte additive on the electrochemical behavior of lead acid battery [J]. Journal of Power Sources, 2009, 187(2): 605−612.

[4] MAO Jian-su, MA Lan, LIANG Jing. Changes in functions, forms, and locations of lead during its anthropogenic flows to provide

services [J]. Transactions of Nonferrous Metals Society of China, 2014, 24(1): 233−242.
[5] KARAMI H, KARIMI M, HAGHDAR S, SADEGHI A, MIR-GHASEMI R, MAHDI-KHANI S. Synthesis of lead oxide nanoparticles by sonochemical method and its application as cathode and anode of lead-acid batteries [J]. Materials Chemistry and Physics, 2008, 108(2−3): 337−344.
[6] CRUZ M, HERNÁN L, MORALES J, SÁNCHEZ L. Spray pyrolysis as a method for preparing PbO coatings amenable to use in lead-acid batteries [J]. Journal of Power Sources, 2002, 108(1−2): 35−40.
[7] NING Peng, PAN Jun-qing, LI Xue, ZHOU Yue, CHEN Jian-feng, WANG Jie-xin. Accelerated desulphurization of waste lead battery paste in a high-gravity rotating packed bed [J]. Chemical Engineering and Processing: Process Intensification, 2016, 104: 148−153.
[8] LIANG Jing, MAO Jian-su. A dynamic analysis of environmental losses from anthropogenic lead flow and their accumulation in China [J]. Transactions of Nonferrous Metals Society of China, 2014, 24(4): 1125−1133.
[9] PAN Jun-qing, SUN Yan-zhi, LI Wei, KNIGHT J, MANTHIRAM A. A green lead hydrometallurgical process based on a hydrogen-lead oxide fuel cell [J]. Nature Communications, 2013, 4: 2178.
[10] LYAKOV N K, ATANASOVA D A, VASSILEV V S, HARALAMPIEV G A. Desulphurization of damped battery paste by sodium carbonate and sodium hydroxide [J]. Journal of Power Sources, 2007, 171: 960−965.
[11] ZHU Xin-feng, YANG Jia-kuan, GAO Lin-xia, LIU Jian-wen, YANG Dan-ni, SUN Xiao-juan, ZHANG Wei, WANG Qin, LI Lei, HE Dong-sheng, KUMAR R V. Preparation of lead carbonate from spent lead paste via chemical conversion [J]. Hydrometallurgy, 2013, 134−135(3): 47−53.
[12] YANAKIEVA V P, HARALAMPIEV G A, LYAKOV N K. Desulphurization of the damped lead battery paste with potassium carbonate [J]. Journal of Power Sources, 2000, 85(1): 178−180.
[13] LIANG Jing, MAO Jian-su. Lead anthropogenic transfer and transformation in China [J]. Transactions of Nonferrous Metals Society of China, 2015, 25(4): 1262−1270.
[14] KARAMI H, KARIMI M A, HAGHDAR S. Synthesis of uniform nano-structured lead oxide by sonochemical method and its application as cathode and anode of lead-acid batteries [J]. Materials Research Bulletin, 2008, 43(11): 3054−3065.
[15] ZHU Xin-feng, HE Xiong, YANG Jia-kuan, GAO Lin-xia, LIU Jian-wen, YANG Dan-ni, SUN Xiao-juan, ZHANG Wei, WANG Qin, KUMAR R V. Leaching of spent lead acid battery paste components by sodium citrate and acetic acid [J]. Journal of Hazardous Materials, 2013, 250-251(8): 387−396.
[16] ZHANG Jun-feng, YI Liang, YANG Liu-chun, HUANG Yan, ZHOU Wen-fang, BIAN Wen-jing. A new pre-desulphurization process of damped lead battery paste with sodium carbonate based on a “surface update” concept [J]. Hydrometallurgy, 2016, 160: 123−128.
[17] CHEN Wei-ping, ZENG Yue, YANG Xia, CHEN Xin-lan, JING Yan-bo. Acid electrolytic treatment process of scrap battery sludge [J]. Transactions of Nonferrous Metals Society of China 1997, 7(4): 138−142.
[18] SONMEZ M S, KUMAR R V. Leaching of waste battery paste components. Part 1: Lead citrate synthesis from PbO and PbO_2 [J]. Hydrometallurgy, 2009, 95(1−2): 53−60.
[19] SONMEZ M S, KUMAR R V. Leaching of waste battery paste components. Part 2: Leaching and desulphurisation of $PbSO_4$ by citric acid and sodium citrate solution [J]. Hydrometallurgy, 2009, 95(1−2): 82−86.
[20] AHN J G, HAI H T, KIM D J, PARK J S, KIM S B. Direct synthesis of nickel powders from NiO slurry by hydrothermal hydrogen reduction process [J]. Hydrometallurgy, 2010, 102: 101−104.
[21] GAO Guo, QIU Pei-yu, QIAN Qi-rong, ZHOU Na, WANG Kan, SONG Hua, FU Hua-lin, CUI Da-xiang. PEG-200-assisted hydrothermal method for the controlled-synthesis of highly dispersed hollow Fe_3O_4 nanoparticles [J]. Journal of Alloys and Compounds, 2013, 574(27): 340−344.
[22] MA Fei-xiang, SUN Xue-yin, HE Kai, JIANG Jian-tang, ZHEN Liang, XU Cheng-yan. Hydrothermal synthesis, magnetic and electromagnetic properties of hexagonal Fe_3O_4 microplates [J]. Journal of Magnetism and Magnetic Materials, 2014, 361: 161−165.
[23] CHEN Wei-ping. New technology of hydrometallurgical recovering lead from waste battery slurry [J]. Journal of Hunan University (Natural Sciences), 1996, 23(6): 111−116. (in Chinese)
[24] QIU Den-fen, KE Chang-mei, WANG Qian, CHEN Shan, LIU Fang-fang. Research progress of reduction technology for PbO_2 from spent lead acid battery [J]. Inorganic Chemicals Industry, 2014, 46(3): 15−18. (in Chinese)

基于水热还原转化从废铅膏中回收铅的清洁工艺

刘伟锋[1,2]，邓循博[1]，张杜超[1]，杨天足[1]，陈 霖[1]

1. 中南大学 冶金与环境学院，长沙 410083；
2. 河南豫光金铅集团有限责任公司，济源 459000

摘 要：提出一种环境友好、节能的新方法从废铅膏中回收铅。首先在水热条件下，通过葡萄糖将废铅膏中的二氧化铅彻底还原，详细研究反应时间、葡萄糖过量系数、温度和 pH 值对水热还原过程的影响，在最优条件，即温度 175 °C、时间 120 min、葡萄糖过量系数 3.0 和 pH 5.5，二氧化铅还原率达到 99.9%，还原渣中只有 $PbO·PbSO_4$ 和 $PbSO_4$ 两种物相。随后，还原渣在氢氧化钠溶液中进行脱硫转化，脱硫率达到 99.40%，脱硫渣中铅主要以 $3PbO·H_2O$ 物相存在。

关键词：废铅膏；水热还原；葡萄糖；脱硫转化

(Edited by Bing YANG)